Eur. Phys. J. B **44**, 401–413 (2005)
DOI: 10.1140/epjb/e2005-00139-x

THE EUROPEAN PHYSICAL JOURNAL B

Electron quasi-confined-optical-phonon interactions in wurtzite GaN/AlN quantum wells

L. Li, D. Liu, and J.-J. Shi[a]

State Key Laboratory for Mesoscopic Physics, and School of Physics, Peking University, Beijing 100871, P.R. China

Received 28 September 2004 / Received in final form 18 January 2005
Published online 30 May 2005 –

Abstract. The equation of motion for the p-polarization field in a wurtzite GaN/AlN multilayer heterostructure is solved for the quasi-confined-optical-phonon modes based on the dielectric-continuum model and Loudon's uniaxial crystal model. The polarization eigenvector, the dispersion relation of the quasi-confined-optical-phonon modes and the electron-quasi-confined-phonon interaction Fröhlich-like Hamiltonian are derived. The analytical formulas can be directly applied to single/multiple quantum wells (QW's) and superlattices. The electron-quasi-confined-phonon coupling functions are investigated for a given AlN/GaN/AlN single QW with full account of the strains of the QW structures and the anisotropy effect of wurtzite crystals. We find that there are two kinds of quasi-confined-optical-phonon modes in the GaN/AlN QW's: the GaN-layer quasi-confined-optical-phonon modes and the AlN-layer quasi-confined-optical-phonon modes. There are infinite quasi-confined-optical-phonon branches, labelled by a quantum number n ($n = 1, 2, \ldots$), with definite symmetry with respect to the center of the AlN/GaN/AlN single QW for a given phonon wave number $q_\perp$. The dispersions of the quasi-confined-optical-phonon modes with smaller n are more obvious than the ones with larger n. Moreover, the modes with smaller n are much more important for their electron-quasi-confined-phonon interactions than those with larger n. In most cases, it is enough to consider the modes with $n \leq 8$ for the electron-quasi-confined-phonon interactions in a single GaN/AlN QW. The higher frequency modes are more significant than the lower ones. The long-wavelength quasi-confined-optical-phonon modes are much more important for the electron-quasi-confined-phonon interactions. The GaN-layer quasi-confined-optical-phonon energies and their electron-quasi-confined-phonon interaction strength are markedly increased due to the strains of the QW structures. The influence of the strains on the the AlN-layer electron-quasi-confined-phonon interactions can be ignored.

PACS. 78.67.De Quantum wells – 63.20.Dj Phonon states and bands, normal modes, and phonon dispersion – 63.20.Kr Phonon-electron and phonon-phonon interactions – 63.22.+m Phonons or vibrational states in low-dimensional structures and nanoscale materials

1 Introduction

In the past decade, the investigation of the optical, electronic, and lattice dynamical properties of quantum heterostructures based on the hexagonal wurtzite group-III nitrides InN, GaN, AlN and their ternary compounds with direct wide-band-gaps in the region of $1.9 \sim 6.2$ eV has been highly developed due to their promising potential for optoelectronic device applications, particularly for high-brightness blue/green light emitting diodes (LED's) and laser diodes (LD's) [1–14]. The quantum heterostructures, which are composed of the different III-V nitrides, naturally form quantum wells (QW's) of the electron or hole along the [0001] direction (c axis) of wurtzite crystal due to the different optical bandgaps of the constituents (please refer to Figs. 5 and 41 of Ref. [3]). The interests and scope of research in this field are increasing day after day. The group-III nitrides usually crystallize in wurtzite structure. Their phonon spectra are much more complex due to anisotropy of the crystal structure compared with phonons in cubic crystals [15–22]. It has been known that, at room and higher temperatures, the electron-phonon interactions and scattering play an important role for various properties of polar semiconductor quantum heterostructures, including hot-electron relaxation rates, interband transition rates, room-temperature exciton lifetimes, and many other optical and transport properties. Hence the understanding of lattice dynamics and electron-phonon interactions in wurtzite quantum heterostructures has attracted much attention.

In recent years, some optoelectronic devices composed of the strained GaN/AlN quantum heterostructures, such as photoconductive detectors, photodiodes,

[a] e-mail: jjshi@pku.edu.cn

field effect transistors, LED's and LD's, have been realized [2,3,6]. The strained GaN/AlN quantum heterostructures thus become a very active research object. Based on the dielectric-continuum (DC) model [15] and Loudon's uniaxial crystal model [23,24], the polar optical-phonons in wurtzite GaN/AlN single heterojunctions, single QW's, and infinite superlattices (SL's) have been examined theoretically in references [12–14]. The electron-optical-phonon scattering in wurtzite crystals and single QW's was investigated in references [25,26]. The polaron properties of III-V nitride compounds were studied in references [27–29]. The polar optical-phonons and their interactions with electrons in GaN/AlN quantum dots (QD's) were also treated in references [30–32]. Angular dispersion of polar phonons and Raman scattering due to extraordinary phonons in wurtzite GaN/AlN SL's were investigated in references [33,34]. The experimental results of references [33,34] were found to be in good agreement with the calculations based on the DC model, which confirmed the accuracy of the DC model for the description of the lattice dynamic properties of wurtzite QW's and SL's. The LO phonon-assisted luminescence of the shallow donor-bound excitons and free excitons in the GaN films was also investigated at different temperatures [35]. With Raman scattering, Bergman et al. [36] investigated phonon lifetimes in wurtzite AlN and GaN; Alexson et al. [37] further studied the confined phonons and the phonon-mode properties of wurtzite III-V nitrides.

It is well known that there are two kinds of important optical-phonon modes in a bulk wurtzite crystal [23,24]. One is the so-called ordinary phonons. Their polarization modes are purely transverse modes (s-polarization modes). They are not accompanied by the appearance either of a surface polarization charge or a bulk one. Hence the electron does not couple to the s-polarization modes [15]. We will not discuss them in this paper. The other is the extraordinary phonons (p-polarization modes), for which the orientation of the electric field $\overrightarrow{E}$ and the polarization vector $\overrightarrow{P}$ with respect to the phonon wave vector $\overrightarrow{q} = (\overrightarrow{q}_{\perp}, q_{\rm z})$ and the c axis is more complicated. Here the subscripts $\perp$ and z denote the perpendicular-direction and the parallel-direction of the z (c) axis. Generally, the p-polarization modes can give rise to a surface polarization charge in a wurtzite quantum heterostructure and will be discussed in detail in the present paper.

Recently, Shi [9–11] solved the p-polarized interface-optical-phonon modes and the propagating-optical-phonon modes in an arbitrary wurtzite quasi-two-dimensional (Q2 D) multilayer heterostructure based on the DC model [15] and Loudon's uniaxial crystal model [23,24]. Five distinct types of optical phonon modes have been confirmed. The quasi-confined-optical-phonon modes, the propagating-optical-phonon modes, the interface-optical-phonon modes, the half-space-optical-phonon modes and the exactly-confined-optical-phonon modes, were found to coexist in a wurtzite Q2D multilayer heterostructure. The Fröhlich-like Hamiltonian due to the electron interactions with the interface-optical-phonon and propagating-optical-phonon modes in wurtzite Q2D multiple quantum wells (MQW's) or SL's have also been derived and discussed in references [9–11]. To the best of our knowledge, the properties of the other three modes have not been fully understood up to now. The purpose of the present paper is to solve the quasi-confined-optical-phonon modes and to derive the electron-quasi-confined-phonon interaction Fröhlich-like Hamiltonian in a wurtzite Q2D GaN/AlN multilayer heterostructure.

The paper is organized as follows. In Section 2, the equation of motion for the p-polarization field in an arbitrary wurtzite Q2D multilayer heterostructure is solved. The polarization eigenvector and the dispersion relation of the quasi-confined-optical-phonon modes are given. In Section 3, the electron-quasi-confined-phonon interaction Fröhlich-like Hamiltonian are derived. In Section 4, the dispersion relations and the electron-quasi-confined-phonon coupling functions are calculated numerically and discussed for a chosen AlN/GaN/AlN single QW. Finally, the main conclusions obtained in this paper are summarized in Section 5.

2 Quasi-confined-optical-phonon modes in a wurtzite GaN/AlN multilayer heterostructure

Let us now consider an arbitrary wurtzite Q2D GaN/AlN multilayer heterostructure with the AlN layer labelled by $j = 0, 2, 4, \ldots, N+1$ and the GaN layer denoted by $j = 1, 3, 5, \ldots, N$. The $j = 0$ and $N+1$ layers are semi-infinite in thickness. The heterointerfaces are located at $z = z_0, z_1, \ldots, z_{\rm N}$ with the z axis along the [0001] direction of wurtzite crystal. Following a procedure analogous to that of reference [9], the general solutions of the p-polarization fields can be obtained.

According to the different values of $q_{\rm z,j}$, we have two types of quasi-confined-optical-phonon modes: the GaN-layer quasi-confined-optical-phonon modes with the phonon wave number $q_{\rm z}$ purely real (imaginary) in the GaN (AlN) layer and the AlN-layer quasi-confined-optical-phonon modes with the phonon wave number $q_{\rm z}$ purely real (imaginary) in the AlN (GaN) layer.

2.1 GaN-layer quasi-confined-optical-phonon modes

According to the equations (2.14) and (2.19) of reference [9], the GaN-layer quasi-confined-optical-phonon solutions ($j = 1, 3, 5, \ldots, N$) can be written as

$$P_{\perp}^{(\rm j)}(z) = C\left[A_{\rm j}e^{iq_{\rm z,j}(z-z_{\rm j})} + B_{\rm j}e^{-iq_{\rm z,j}(z-z_{\rm j})}\right],$$
$$P_{\rm z}^{(\rm j)}(z) = \gamma_{\rm j}C\left[A_{\rm j}e^{iq_{\rm z,j}(z-z_{\rm j})} - B_{\rm j}e^{-iq_{\rm z,j}(z-z_{\rm j})}\right]. \quad (1)$$

Here $q_{\rm z,j}$ is purely real. On the contrary, $q_{\rm z,j}$ becomes imaginary in the AlN layers ($j = 0, 2, 4, \ldots, N+1$) and can

be substituted by $iq_{\mathrm{z,j}}$. We thus have the quasi-confined-optical-phonon solutions in the AlN layers as follows

$$P_{\perp}^{(\mathrm{j})}(z) = C\left[A_{\mathrm{j}}e^{-q_{\mathrm{z,j}}(z-z_{\mathrm{j}})} + B_{\mathrm{j}}e^{q_{\mathrm{z,j}}(z-z_{\mathrm{j}})}\right],$$
$$P_{\mathrm{z}}^{(\mathrm{j})}(z) = i\gamma_{\mathrm{j}}C\left[A_{\mathrm{j}}e^{-q_{\mathrm{z,j}}(z-z_{\mathrm{j}})} - B_{\mathrm{j}}e^{q_{\mathrm{z,j}}(z-z_{\mathrm{j}})}\right]. \quad (2)$$

In equations (1) and (2), C is a constant determined by equation (16), and γ_{j} is defined as

$$\gamma_{\mathrm{j}} \equiv \frac{q_{\mathrm{z,j}}\chi_{\mathrm{z,j}}(\omega)}{q_{\perp}\chi_{\perp,\mathrm{j}}(\omega)}. \quad (3)$$

Here χ is the lattice susceptibility. Using the electrostatic boundary conditions, i.e., equations (2.16) and (2.17) of reference [9] at the $z = z_{\mathrm{j}}$ interface, we have the following matrix relation relating the successive coefficients $A_{\mathrm{j+1}}$ and $B_{\mathrm{j+1}}$:

$$\begin{pmatrix} A_{\mathrm{j+1}} \\ B_{\mathrm{j+1}} \end{pmatrix} = M_{\mathrm{j}} \begin{pmatrix} A_{\mathrm{j}} \\ B_{\mathrm{j}} \end{pmatrix}, \qquad j = 0, 1, \ldots, N, \quad (4)$$

where $A_0 = 0$ and $B_{N+1} = 0$ in the AlN layer. The transfer matrix M_{j} from the layer j to the layer $j+1$ is defined as

$$M_j = \frac{\beta_{\mathrm{j,j+1}}}{2}\begin{pmatrix} \sigma_- e^{-q_{\mathrm{z,j+1}}d_{\mathrm{j+1}}} & \sigma_+ e^{-q_{\mathrm{z,j+1}}d_{\mathrm{j+1}}} \\ \sigma_+ e^{q_{\mathrm{z,j+1}}d_{\mathrm{j+1}}} & \sigma_- e^{q_{\mathrm{z,j+1}}d_{\mathrm{j+1}}} \end{pmatrix}, \quad (j = 1, 3, 5, \ldots, N). \quad (5)$$

The corresponding result for $j = 0, 2, 4, \ldots, N-1$ is

$$M_j = \frac{\beta_{\mathrm{j,j+1}}}{2}\begin{pmatrix} \sigma_+ e^{iq_{\mathrm{z,j+1}}d_{\mathrm{j+1}}} & \sigma_- e^{iq_{\mathrm{z,j+1}}d_{\mathrm{j+1}}} \\ \sigma_- e^{-iq_{\mathrm{z,j+1}}d_{\mathrm{j+1}}} & \sigma_+ e^{-iq_{\mathrm{z,j+1}}d_{\mathrm{j+1}}} \end{pmatrix}, \quad (6)$$

where $d_{\mathrm{j+1}} \equiv z_{\mathrm{j+1}} - z_{\mathrm{j}}$ is the thickness of the layer $j+1$, and $\sigma_{\pm}$ is given by

$$\sigma_{\pm} = 1 \pm i\alpha_{\mathrm{j,j+1}}. \quad (7)$$

Here $\alpha_{\mathrm{j,j+1}}$ and $\beta_{\mathrm{j,j+1}}$ are defined as

$$\alpha_{\mathrm{j,j+1}} \equiv \frac{q_{\mathrm{z,j}}\epsilon_{\mathrm{z,j}}(\omega)}{q_{\mathrm{z,j+1}}\epsilon_{\mathrm{z,j+1}}(\omega)},$$
$$\beta_{\mathrm{j,j+1}} \equiv \frac{\chi_{\perp,\mathrm{j+1}}(\omega)}{\chi_{\perp,\mathrm{j}}(\omega)}, \quad (8)$$

where ϵ is the lattice dielectric function. Moreover, the matrix relation relating the coefficients in the $j = 0$ layer and the $j = N+1$ layer can be written as

$$\begin{pmatrix} A_{\mathrm{N+1}} \\ 0 \end{pmatrix} = M_{\mathrm{tot}} \begin{pmatrix} 0 \\ B_0 \end{pmatrix}, \quad (9)$$

with

$$M_{\mathrm{tot}} = \begin{pmatrix} M_{11} & M_{12} \\ M_{21} & M_{22} \end{pmatrix} = M_{\mathrm{N}}M_{\mathrm{N-1}}\cdots M_0. \quad (10)$$

We can obtain from equation (9) the following dispersion relation for the GaN-layer quasi-confined-optical-phonon modes in a wurtzite Q2D GaN/AlN multilayer heterostructure:

$$M_{22} = 0. \quad (11)$$

This equation is the most general expression of the GaN-layer quasi-confined-optical-phonon dispersion relation for a wurtzite Q2D GaN/AlN multilayer system.

As an important special case of Q2D GaN/AlN multilayer heterostructures, let us now further discuss equation (11) for an AlN/GaN/AlN single QW. For convenience, we will use index 1 for the QW material GaN and index 2 for the surrounding material AlN. We can obtain from equation (11) the following dispersion relation for the GaN-layer quasi-confined-optical-phonon modes,

$$q_{\mathrm{z},1}d = \arctan\left[2\left(\sqrt{\frac{\kappa(0)}{\kappa(1)}} - \sqrt{\frac{\kappa(1)}{\kappa(0)}}\right)^{-1}\right] + n\pi, \quad n = 1, 2, 3, \ldots, \quad (12)$$

where

$$q_{\mathrm{z},1} = \sqrt{\left|\frac{\epsilon_{\perp,1}(\omega)}{\epsilon_{\mathrm{z},1}(\omega)}\right|}q_{\perp}, \qquad (q_{\perp} > 0), \quad (13)$$

and

$$\kappa(m) = |\epsilon_{\perp,m}\epsilon_{\mathrm{z,m}}| = \left|\epsilon_{\perp,m}^{\infty}\frac{\omega^2 - \omega_{\perp,L_m}^2}{\omega^2 - \omega_{\perp,T_m}^2}\epsilon_{\mathrm{z,m}}^{\infty}\frac{\omega^2 - \omega_{z,L_m}^2}{\omega^2 - \omega_{z,T_m}^2}\right|. \quad (14)$$

Here d is the thickness of GaN layer, ϵ^{∞} denotes the optical dielectric constant, $\omega_{\perp,L}$ and $\omega_{z,L}$ ($\omega_{\perp,T}$ and $\omega_{z,T}$) are the zone center LO (TO) phonon frequencies, and n is a quantum number for the nth quasi-confined-optical-phonon mode in the GaN layer. Generally, equation (12) has an infinite number of solutions with definite symmetry with respect to the symmetric center of the QW structure for a given phonon wave number $q_{\perp}$ (see Figs. 2 and 3). Moreover, we can prove that equation (12) is equivalent to equations (20) and (21) of reference [14].

According to equations (1) and (2), we can obtain the two-dimensional p-polarization eigenvector $\overrightarrow{\pi}(q_{\perp}, z) \equiv (P_{\perp}, P_{\mathrm{z}})$ for the GaN-layer quasi-confined-optical-phonon modes as

$$\overrightarrow{\pi}(q_{\perp}, z) = C\begin{cases} Q_1, & z < z_0, \\ Q_{2,\mathrm{GaN}}, & z_{\mathrm{j-1}} < z < z_{\mathrm{j}},\ j = 1, 3\ldots, N, \\ Q_{2,\mathrm{AlN}}, & z_{\mathrm{j-1}} < z < z_{\mathrm{j}}, \\ & \quad j = 2, 4\ldots, N-1, \\ Q_3, & z > z_{\mathrm{N}}. \end{cases} \quad (15)$$

$$Q_1(q_{\perp}, z) = e^{q_{\mathrm{z},0}(z-z_0)}[1, -i\gamma_0],$$
$$Q_{2,\mathrm{GaN}}(q_{\perp}, z) = \left[\left(A_{\mathrm{j}}e^{iq_{\mathrm{z,j}}(z-z_{\mathrm{j}})} + B_{\mathrm{j}}e^{-iq_{\mathrm{z,j}}(z-z_{\mathrm{j}})}\right), \gamma_{\mathrm{j}}\left(A_{\mathrm{j}}e^{iq_{\mathrm{z,j}}(z-z_{\mathrm{j}})} - B_{\mathrm{j}}e^{-iq_{\mathrm{z,j}}(z-z_{\mathrm{j}})}\right)\right],$$
$$Q_{2,\mathrm{AlN}}(q_{\perp}, z) = \left[\left(A_{\mathrm{j}}e^{-q_{\mathrm{z,j}}(z-z_{\mathrm{j}})} + B_{\mathrm{j}}e^{q_{\mathrm{z,j}}(z-z_{\mathrm{j}})}\right), i\gamma_{\mathrm{j}}\left(A_{\mathrm{j}}e^{-q_{\mathrm{z,j}}(z-z_{\mathrm{j}})} - B_{\mathrm{j}}e^{q_{\mathrm{z,j}}(z-z_{\mathrm{j}})}\right)\right],$$
$$Q_3(q_{\perp}, z) = A_{\mathrm{N+1}}e^{-q_{\mathrm{z,N+1}}(z-z_{\mathrm{N}})}[1, i\gamma_{\mathrm{N+1}}].$$

The coefficient C in equation (15) can be determined by the orthonormality condition, i.e., equation (2.37) of reference [9], as follows:

$$C = \sqrt{\frac{1}{\Lambda}}, \tag{16}$$

with

$$\begin{aligned}\Lambda = Q_{0,+}/(2q_{\mathrm{z,0}}) + \sum_{j=1,3,5\cdots}^{N} \{(|A_j|^2 + |B_j|^2) d_j Q_{\mathrm{j},+} \\ + [A_j^* B_j i(1 - e^{2iq_{\mathrm{z,j}}d_{\mathrm{j}}})/(2q_{\mathrm{z,j}}) \\ - A_j B_j^* i(1 - e^{-2iq_{\mathrm{z,j}}d_{\mathrm{j}}})/(2q_{\mathrm{z,j}})] Q_{\mathrm{j},-}\} \\ + \sum_{j=2,4,6\cdots}^{N-1} \{[|A_j|^2 (e^{2q_{\mathrm{z,j}}d_j} - 1) \\ + |B_j|^2 (1 - e^{-2q_{\mathrm{z,j}}d_j})] Q_{\mathrm{j},+}/(2q_{\mathrm{z,j}}) + (A_j^* B_j + A_j B_j^*) d_j Q_{\mathrm{j},-}\} \\ + |A_{N+1}|^2 Q_{\mathrm{N+1},+}/(2q_{\mathrm{z,N+1}}).\end{aligned} \tag{17}$$

Here A_j^* and B_j^* are the complex conjugates of A_j and B_j, and $Q_{\mathrm{j},\pm}$ is defined as

$$Q_{\mathrm{j},\pm} \equiv \frac{\eta_{\perp,\mathrm{j}}(\omega)}{\omega_{\perp,\mathrm{pj}}^2} \pm \gamma_{\mathrm{j}}^2 \frac{\eta_{\mathrm{z,j}}(\omega)}{\omega_{\mathrm{z,pj}}^2}.$$

The definitions of $\eta_{\mathrm{j}}(\omega)$ and ω_{pj} are given in reference [19].

2.2 AlN-layer quasi-confined-optical-phonon modes

Similar to Section 2.1, the solutions of the AlN-layer quasi-confined-optical-phonon modes ($j = 0, 2, 4, \ldots, N+1$) are as follows:

$$\begin{aligned}P_{\perp}^{(\mathrm{j})}(z) &= C' \left[A_{\mathrm{j}} e^{iq_{\mathrm{z,j}}(z - z_{\mathrm{j}})} + B_{\mathrm{j}} e^{-iq_{\mathrm{z,j}}(z - z_{\mathrm{j}})}\right], \\ P_{\mathrm{z}}^{(\mathrm{j})}(z) &= \gamma_{\mathrm{j}} C' \left[A_{\mathrm{j}} e^{iq_{\mathrm{z,j}}(z - z_{\mathrm{j}})} - B_{\mathrm{j}} e^{-iq_{\mathrm{z,j}}(z - z_{\mathrm{j}})}\right].\end{aligned} \tag{18}$$

The corresponding solutions in the GaN layers ($j = 1, 3, 5, \ldots, N$) can be written as

$$\begin{aligned}P_{\perp}^{(\mathrm{j})}(z) &= C' \left[A_{\mathrm{j}} e^{-q_{\mathrm{z,j}}(z - z_{\mathrm{j}})} + B_{\mathrm{j}} e^{q_{\mathrm{z,j}}(z - z_{\mathrm{j}})}\right], \\ P_{\mathrm{z}}^{(\mathrm{j})}(z) &= i\gamma_{\mathrm{j}} C' \left[A_{\mathrm{j}} e^{-q_{\mathrm{z,j}}(z - z_{\mathrm{j}})} - B_{\mathrm{j}} e^{q_{\mathrm{z,j}}(z - z_{\mathrm{j}})}\right].\end{aligned} \tag{19}$$

The transfer matrix M_{j} for $j = 1, 3, 5, \ldots, N$ is given by

$$M_{\mathrm{j}} = \frac{\beta_{\mathrm{j,j+1}}}{2} \begin{pmatrix} \sigma_+ e^{iq_{\mathrm{z,j+1}}d_{\mathrm{j+1}}} & \sigma_- e^{iq_{\mathrm{z,j+1}}d_{\mathrm{j+1}}} \\ \sigma_- e^{-iq_{\mathrm{z,j+1}}d_{\mathrm{j+1}}} & \sigma_+ e^{-iq_{\mathrm{z,j+1}}d_{\mathrm{j+1}}} \end{pmatrix}. \tag{20}$$

The corresponding result for $j = 0, 2, 4, \ldots, N-1$ can be written as

$$M_{\mathrm{j}} = \frac{\beta_{\mathrm{j,j+1}}}{2} \begin{pmatrix} \sigma_- e^{-q_{\mathrm{z,j+1}}d_{\mathrm{j+1}}} & \sigma_+ e^{-q_{\mathrm{z,j+1}}d_{\mathrm{j+1}}} \\ \sigma_+ e^{q_{\mathrm{z,j+1}}d_{\mathrm{j+1}}} & \sigma_- e^{q_{\mathrm{z,j+1}}d_{\mathrm{j+1}}} \end{pmatrix}. \tag{21}$$

For simplicity, let us now consider a symmetric wurtzite GaN/AlN Q2D multilayer heterostructure with the same thickness d for the GaN and AlN layers embedded in the two semi-infinite AlN layers. We can easily find that there are two types of the AlN-layer quasi-confined-optical-phonon modes: the symmetric and antisymmetric modes with respect to the center of the whole structure, i.e., the center of the layer $m \equiv (N+1)/2$. According to reference [13], the following relationships between the coefficients A_j and B_j in the $j = 0$ ($j = m$) layer can be found,

$$\begin{aligned}A_0 &= (-1)^s B_0 e^{-iq_{\mathrm{z,0}}Nd}, \\ A_m &= (-1)^s B_m e^{-q_{\mathrm{z,m}}d},\end{aligned} \tag{22}$$

where $s = 0$ ($s = 1$) is for the symmetric (antisymmetric) modes.

Based on the electrostatic boundary conditions, we have the following relation,

$$\begin{pmatrix} A_{\mathrm{m}} \\ B_{\mathrm{m}} \end{pmatrix} = M'_{\mathrm{tot}} \begin{pmatrix} A_0 \\ B_0 \end{pmatrix}, \tag{23}$$

where

$$M'_{\mathrm{tot}} = \begin{pmatrix} M'_{11} & M'_{12} \\ M'_{21} & M'_{22} \end{pmatrix} = M_{\frac{N-1}{2}} M_{\frac{N-3}{2}} \cdots M_0. \tag{24}$$

Furthermore, we can derive the following dispersion relation for the AlN-layer quasi-confined-optical-phonon modes from equations (22) and (23),

$$\begin{aligned}e^{-q_{\mathrm{z,m}}d - iq_{\mathrm{z,0}}Nd} M'_{21} - M'_{12} = \\ (-1)^s \left[e^{-iq_{\mathrm{z,0}}Nd} M'_{11} - e^{-q_{\mathrm{z,m}}d} M'_{22}\right].\end{aligned} \tag{25}$$

This equation is the most general expression of the AlN-layer quasi-confined-optical-phonon dispersion relation for our symmetric wurtzite GaN/AlN Q2D multilayer system. For an AlN/GaN/AlN single QW, we can derive the following dispersion relation for the AlN-layer quasi-confined-optical-phonon modes from equation (25),

$$\begin{aligned}q_{\mathrm{z},2}d/2 + \arctan\left[(-1)^{m_1+1} \nu(m_1, m_2) \tanh(q_{\mathrm{z},1}d/2)\right] = n\pi. \\ n = 1, 2, 3, \ldots\end{aligned} \tag{26}$$

Here the index 1 is for the QW material GaN and index 2 for the surrounding material AlN, and n is a quantum number for the nth quasi-confined-optical-phonon mode in the AlN layer. In equation (26), $m_1 = 1, m_2 = 2$ ($m_1 = 2, m_2 = 1$) is for the symmetric (antisymmetric) modes and $\nu(m_1, m_2)$ is defined as,

$$\nu(m_1, m_2) = \frac{\epsilon_{\mathrm{z},\mathrm{m}_1} q_{\mathrm{z},\mathrm{m}_1}}{\epsilon_{\mathrm{z},\mathrm{m}_2} q_{\mathrm{z},\mathrm{m}_2}}. \tag{27}$$

Equation (26) has an infinite number of phonon mode solutions with definite symmetry with respect to the symmetric center of the QW structure for a given phonon wave number $q_{\perp}$ (please refer to Figs. 5 and 6).

From equations (18) and (19), we can obtain the two-dimensional p-polarization eigenvector

$\overrightarrow{\pi}(q_\perp, z) \equiv (P_\perp, P_z)$ for the AlN-layer quasi-confined-optical-phonon modes as follows:

$$\overrightarrow{\pi} = C' \begin{cases} Q_1, & z < z_0, \\ Q_{2,\mathrm{GaN}}, & z_{j-1} < z < z_j, \quad j = 1, 3 \ldots, N, \\ Q_{2,\mathrm{AlN}}, & z_{j-1} < z < z_j, \quad j = 2, 4 \ldots, N-1, \\ Q_3, & z > z_N. \end{cases} \tag{28}$$

Here Q_1, $Q_{2,\mathrm{AlN}}$ and Q_3 have the identical forms as functions of the wave number $q_\perp$ and the coordinate z. The functions $Q_1(q_\perp, z)$ and $Q_{2,\mathrm{GaN}}(q_\perp, z)$ are defined as

$$\begin{aligned} Q_1(q_\perp, z) = \Big[& \left(A_j e^{iq_{z,j}(z-z_j)} + B_j e^{-iq_{z,j}(z-z_j)} \right), \\ & \gamma_j \left(A_j e^{iq_{z,j}(z-z_j)} - B_j e^{-iq_{z,j}(z-z_j)} \right) \Big], \\ Q_{2,\mathrm{GaN}}(q_\perp, z) = \Big[& \left(A_j e^{-q_{z,j}(z-z_j)} + B_j e^{q_{z,j}(z-z_j)} \right), \\ & -i\gamma_j \left(-A_j e^{-q_{z,j}(z-z_j)} + B_j e^{q_{z,j}(z-z_j)} \right) \Big]. \end{aligned} \tag{29}$$

The coefficient C' in equation (28) can be determined by the orthonormality condition of the eigenvector $\overrightarrow{\pi}(q_\perp, z)$ as follows:

$$C' = \sqrt{\frac{1}{\Lambda'}}, \tag{30}$$

where Λ' is defined as

$$\begin{aligned} \Lambda' = & (|B_0|^2+1)(z_0+L)Q_{0,+} + \frac{B_0^*}{2iq_{z,o}}[1-e^{-2iq_{z,0}(L+Z_0)}]Q_{0,-} \\ & - \frac{B_0}{2iq_{z,o}}[1-e^{2iq_{z,0}(L+Z_0)}]Q_{0,+} + \sum_{j=1,3,5\cdots}^{N} \{[|A_j|^2(e^{2q_{z,j}d_j}-1) \\ & + |B_j|^2(1-e^{-2q_{z,j}d_j})]Q_{j,+}/(2q_{z,j}) + 2A_jB_jd_jQ_{j,-}\} \\ & + \sum_{j=2,4,6\ldots}^{N-1} \{(|A_j|^2+|B_j|^2)d_jQ_{j,+} \\ & + A_j^*B_ji(1-e^{2iq_{z,j}d_j})/(2q_{z,j}) \\ & - A_jB_j^*i(1-e^{-2iq_{z,j}d_j})/(2q_{z,j})\} \\ & + (|A_{N+1}|^2+|B_{N+1}|^2)(L-z_N)Q_{N+1,+} \\ & + \frac{A_{N+1}B_{N+1}^*}{2iq_{z,N+1}}[e^{-2iq_{z,N+1}(L-Z_N)}-1]Q_{N+1,-} \\ & - \frac{A_{N+1}^*B_{N+1}}{2iq_{z,N+1}}[e^{2iq_{z,N+1}(L-Z_N)}-1]Q_{N+1,+}. \end{aligned} \tag{31}$$

Here $2L$ denotes the total length of the wurtzite Q2D multilayer heterostructure along the z-direction (c axis) with $L \gg (z_N - z_0)$.

3 Electron-quasi-confined-phonon interactions in a wurtzite multilayer heterostructure

The Fröhlich-like Hamiltonian H_{e-ph} due to the electron-quasi-confined-phonon interactions can be obtained by quantizing the energy of interaction of an electron at the position $\overrightarrow{r}$ with the scalar potential produced by the phonons, i.e., $-e\phi(\overrightarrow{r})$ (please refer to Refs. [15,38]). For the two kinds of quasi-confined-optical-phonon modes given in Section 2, we can obtain their electron phonon interaction Hamiltonian in an arbitrary wurtzite Q2D GaN/AlN multilayer heterostructure as follows:

$$\begin{aligned} H_{e-ph} = \sum_n \sum_{\overrightarrow{q}_\perp} & [\hat{a}_n(\overrightarrow{q}_\perp)\Gamma_n(q_\perp, z)e^{i\overrightarrow{q}_\perp \cdot \overrightarrow{\rho}} \\ & + \hat{a}_n^\dagger(\overrightarrow{q}_\perp)\Gamma_n^*(q_\perp, z)e^{-i\overrightarrow{q}_\perp \cdot \overrightarrow{\rho}}]. \end{aligned} \tag{32}$$

We can use the absolute value of the electron-quasi-confined-phonon coupling function $\Gamma_n(q_\perp, z)$ to describe the coupling strength of a single electron located at the position z with the nth quasi-confined-optical-phonon mode.

Based on reference [15] and Section 2, the coupling function $\Gamma_n(q_\perp, z)$ between an electron and the GaN-layer quasi-confined-phonons in an arbitrary wurtzite Q2D GaN/ AlN multilayer heterostructure can be derived as follows:

$$\Gamma_n(q_\perp, z) = C \left(\frac{\hbar e^2}{8A\varepsilon_0\omega_n(q_\perp)} \right)^{1/2} \times \begin{cases} f_1(q_\perp, z), & z < z_0, \\ f_{2,\mathrm{GaN}}(q_\perp, z), & z_{j-1} < z < z_j, \ j = 1, 3, \ldots, N, \\ f_{2,\mathrm{AlN}}(q_\perp, z), & z_{j-1} < z < z_j, \ j = 2, 4, \ldots, N-1, \\ f_3(q_\perp, z), & z > z_N, \end{cases} \tag{33}$$

where A is the cross-sectional area of the heterostructure, and ε_0 is the absolute dielectric constant. The normal frequency $\omega_n(q_\perp)$ of the nth branch of the quasi-confined-optical-phonon modes in the GaN layers can be obtained by solving the dispersion relation equation (11) numerically. The expressions of $f_i(q_\perp, z)$ $(i = 1, 2, 3)$ are given in Appendix A.

The electron-phonon coupling function due to the AlN-layer quasi-confined-optical-phonon modes in a symmetric wurtzite GaN/AlN Q2D multilayer heterostructure can also be obtained, which has an expression similar to equation (33). Please refer to Appendix B.

The analytical expressions given in Section 3 for the electron-quasi-confined-phonon coupling function in an arbitrary wurtzite GaN/AlN Q2D multilayer heterostructure are universal, and can be directly applied to many important Q2D multilayer systems, such as single/multiple QW's and SL's. Moreover, our results are also useful for further investigation of the optical properties and polaron effects of the commonly used GaN-based devices, such as LED's and LD's.

4 Numerical results and discussion

In Sections 2 and 3, we have derived the dispersion equations and the polarization eigenvectors of the quasi-confined-optical-phonon modes in the GaN and AlN layers, and their electron phonon interaction Fröhlich-like

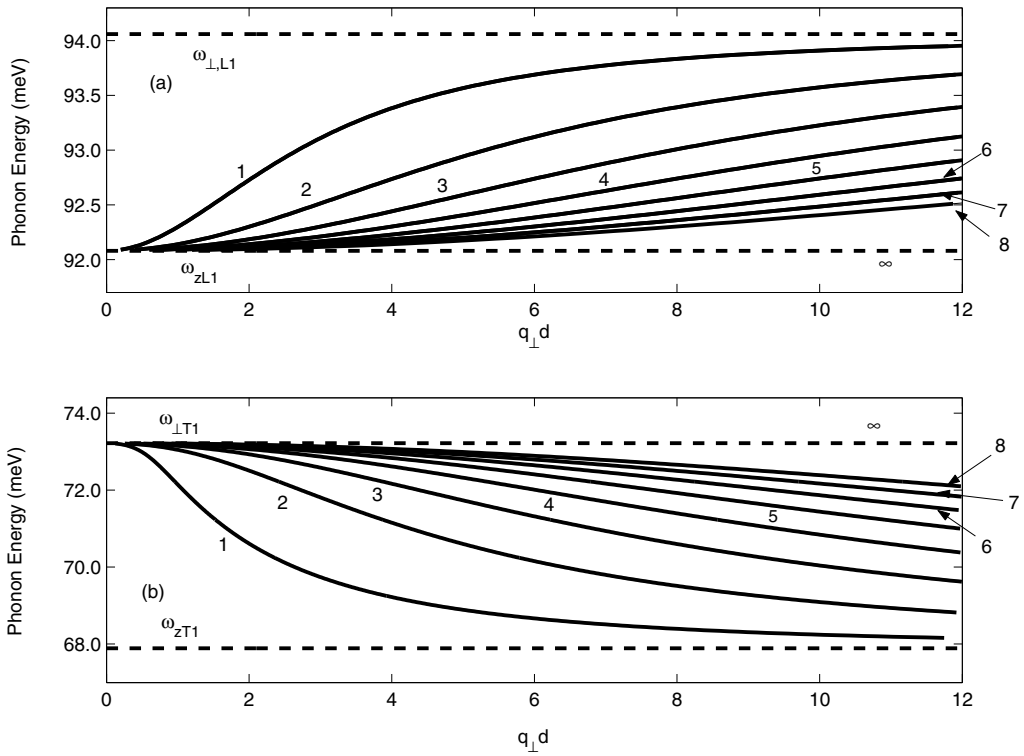

Fig. 1. Dispersion curves of the GaN-layer quasi-confined-optical-phonon modes for a symmetric AlN/GaN/AlN single QW with the GaN well layer thickness of $d = 5$ nm. The numbers next to the curves represent the quantum number n. Here (a) is for the higher frequency modes, (b) for the lower frequency modes, and the strains of the QW structure are included.

Hamiltonian in a general wurtzite GaN/AlN Q2D multilayer heterostructure. However, the corresponding analytical formulas are complicated. In order to see behaviors of the quasi-confined-optical-phonon modes and their interactions with electrons more clearly, we have calculated the quasi-confined-optical-phonon dispersions and their electron-quasi-confined-phonon coupling functions for a symmetric AlN/GaN/AlN single QW. The material parameters used in our calculations are the same as in reference [9].

4.1 GaN-layer quasi-confined-optical-phonon modes and their electron-quasi-confined-phonon interactions

Considering the strains of the QW structure, the dispersion of the GaN-layer quasi-confined-optical-phonon modes in a symmetric AlN/GaN/AlN single QW is shown in Figure 1. We can see from Figure 1 that the GaN-layer quasi-confined-optical-phonon modes exist in the two regions: higher frequency modes between the GaN A_1(LO) and E_1(LO) frequencies, and the lower frequency modes within the region of the GaN A_1(TO) and E_1(TO) frequencies. Furthermore, we can see from Figure 1 that there are infinite quasi-confined-optical-phonon branches with definite symmetry with respect to the middle plane of the QW for a given phonon wave number $q_\perp$ in each range (please refer to Figs. 2 and 3). These branches are denoted by a quantum number n ($n = 1, 2, \ldots, \infty$). Figure 1 also shows that the dispersion of the GaN-layer quasi-confined-optical-phonon modes with smaller n is more dispersive than the modes with larger n. When n goes to infinity, the value of $\hbar\omega_{\perp T1} = 73.22$ (92.08) meV is obtained as a limit in the lower (higher) frequency domain. If $q_\perp \to \infty$, the higher and lower frequency quasi-confined-optical-phonon branches approach the E_1(LO) and A_1(TO) frequencies of GaN material, respectively. Moreover, our calculations also show that, if ignoring the strain of the GaN layer, the dispersion behavior of the quasi-confined-optical-phonon modes is similar to Figure 1. Generally, the strains of the GaN layer will increase the frequency of the quasi-confined-optical-phonon modes.

Figures 2 and 3 show the spatial (z) dependence of the GaN-layer electron-quasi-confined-phonon coupling function $\Gamma(q_\perp, z)$ for the same symmetric single QW structure as in Figure 1. Our calculations indicate that, in most cases, the electron-quasi-confined-phonon interactions are important only for the modes with the small quantum number ($n = 1, 2, \ldots, 8$), and can be ignored for the other modes with the large quantum number. We will thus pay attention to the GaN-layer lower and higher frequency quasi-confined-optical-phonon modes with the quantum number $n = 1, 2, 3, 4$. The results for the $n \geq 5$ modes are similar to those for the $n = 1, 2, 3, 4$ modes and are not shown. Figure 2 indicates that the electron-quasi-confined-phonon interactions with the lower frequency modes are basically localized in the GaN well layer and in the vicinity of the interfaces. Figure 3 shows that the electron-quasi-confined-phonon interactions with the higher frequency

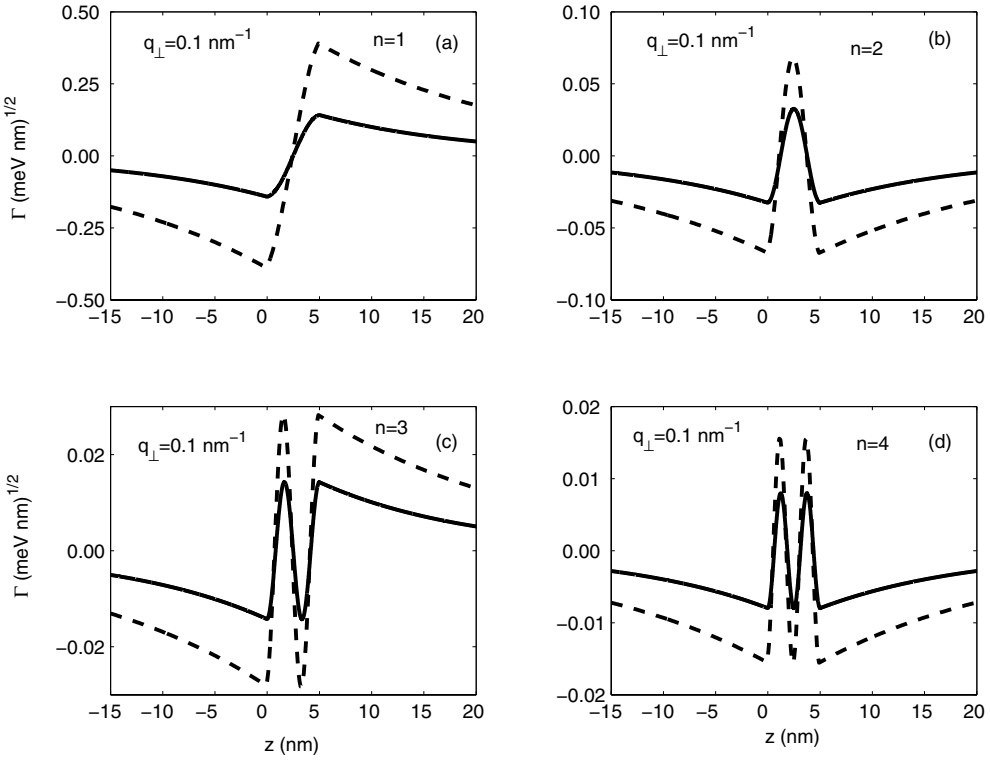

Fig. 2. Spatial dependence of the real part of the coupling function $\Gamma(q_\perp, z)$ divided by $(\hbar e^2/8A\varepsilon_0)^{1/2}$ for the interactions between an electron and the GaN-layer lower frequency quasi-confined-optical-phonon modes with the quantum number $n = 1, 2, 3, 4$ and the wave number $q_\perp = 0.1$ nm^{-1} for the AlN(∞)/GaN(5 nm)/AlN(∞) symmetric single QW. The heterointerfaces are located at $z = 0$ and 5 nm, respectively. The solid (dashed) lines are for the unstrained (strained) QW structure.

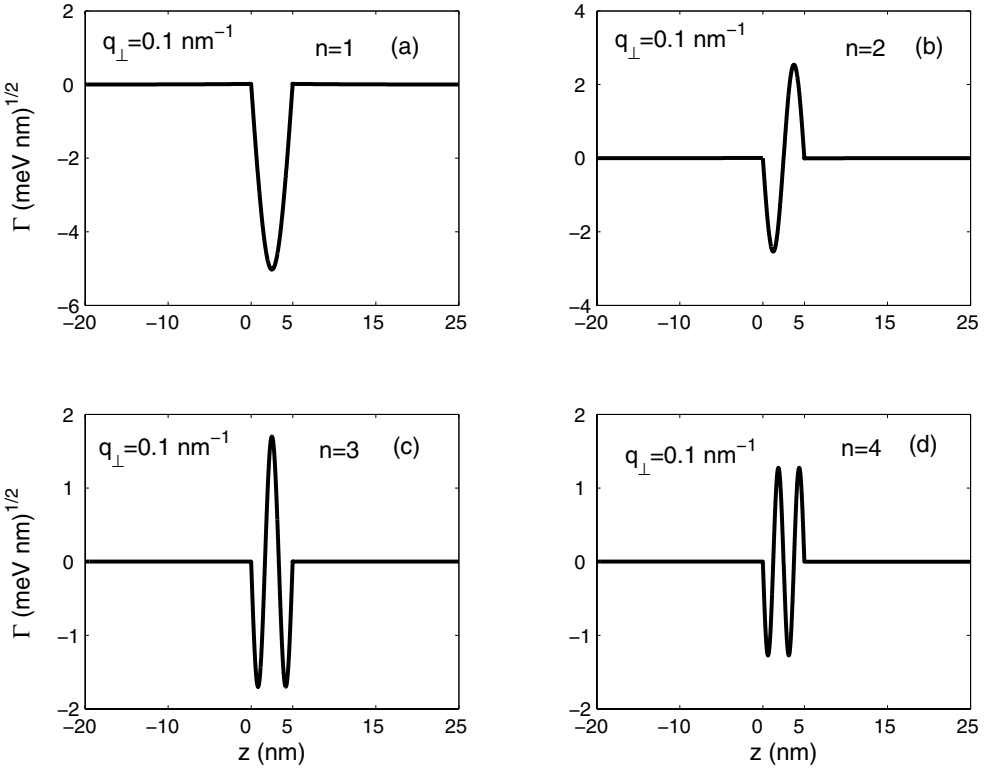

Fig. 3. Same as in Figure 2, but for the higher frequency quasi-confined-optical-phonon modes. Here the strains of the GaN layer are considered.

modes are mainly in the GaN well layer. Moreover, we can see from Figures 2 and 3 that the interaction intensity between an electron and the higher frequency modes is one order of magnitude larger than that between an electron and the lower frequency modes.

Figures 2 and 3 clearly show that the GaN-layer electron-quasi-confined-phonon coupling function $\Gamma(q_\perp, z)$ has exact symmetry with respect to the center of the QW structure at $z = 2.5$ nm for a given quasi-confined-optical-phonon mode. We can see from Figure 2 that the real part of $\Gamma(q_\perp, z)$ is antisymmetric (symmetric) with respect to the center of the QW structure for the $n = 1, 3, \ldots$ ($n = 2, 4, \ldots$) lower frequency modes. On the contrary, the real part of $\Gamma(q_\perp, z)$ is symmetric (antisymmetric) for the $n = 1, 3, \ldots$ ($n = 2, 4, \ldots$) higher frequency modes (please refer to Fig. 3). For the GaN-layer quasi-confined-optical-phonon modes, our calculations indicate that the imaginary part of $\Gamma(q_\perp, z)$ is zero. Figure 2 also indicates that in the lower frequency domain the electron-quasi-confined-phonon interactions have oscillation (exponential attenuation) behavior in the GaN (AlN) layer. With increasing of the quantum number n, the oscillation period of the electron-quasi-confined-phonon coupling function $|\Gamma(q_\perp, z)|$ is reduced for a given $q_\perp$.

Furthermore, we can see from Figure 2 that the strength of the GaN-layer electron-quasi-confined-phonon interactions increase evidently and the oscillation period of the electron-quasi-confined-phonon coupling function $\Gamma(q_\perp, z)$ is not influenced for a given $q_\perp$ if the strains of the QW structure are included. Our calculations also show that the influence of the strains of the QW structure on the the GaN-layer electron-quasi-confined-phonon coupling function can be ignored for the higher frequency modes.

Figure 4 shows the absolute values $|\Gamma(q_\perp, z)|$ as a function of wave number $q_\perp$ for the same QW structure as in Figure 1. According to Figures 2 and 3, we choose the $z = 0$ nm for the lower frequency modes, and $z = 2$ nm for the higher frequency modes. We can see from Figure 4 that $|\Gamma(q_\perp, z)|$ is a complicated function of $q_\perp$. Moreover, Figure 4 also indicates that the long-wavelength quasi-confined-optical-phonon modes are much more important for the electron-quasi-confined-phonon interactions than the short-wavelength ones.

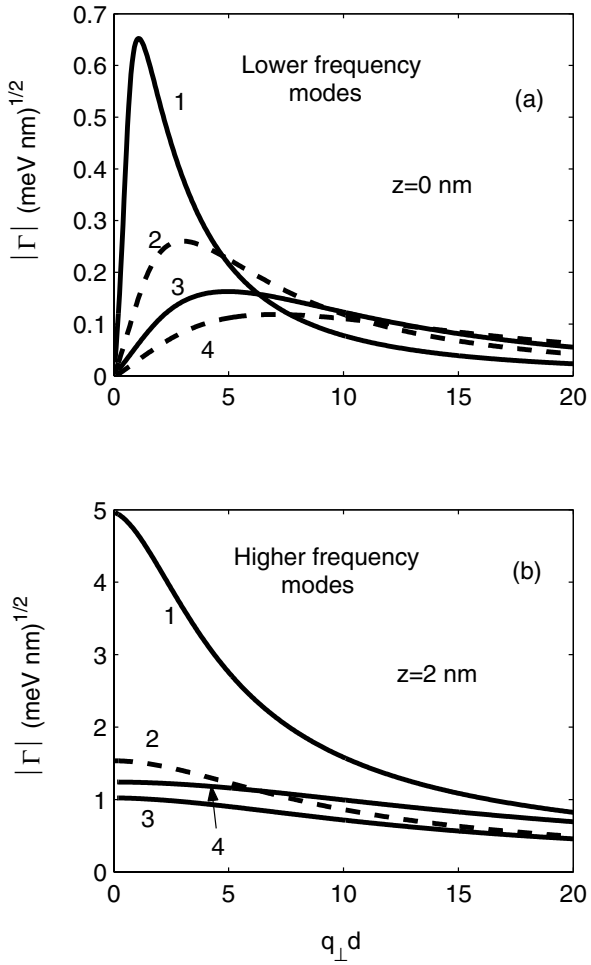

Fig. 4. Absolute values $|\Gamma(q_\perp, z)|$ divided by $(\hbar e^2/8A\varepsilon_0)^{1/2}$ as a function of $q_\perp$ for the same QW structure as in Figure 1. Here (a) and (b) are for the lower and higher frequency modes of the strained QW structure, respectively.

4.2 AlN-layer quasi-confined-optical-phonon modes and their electron-quasi-confined-phonon interactions

Our calculations show that the dispersion behavior of the AlN-layer quasi-confined-optical-phonon modes is similar to that of the GaN-layer quasi-confined-optical-phonon modes. The influence of the strains of the GaN QW layer on the dispersion characteristics of the AlN-layer quasi-confined-optical-phonon modes can be ignored.

Figures 5 and 6 indicate the spatial (z) dependence of the coupling function $\Gamma(q_\perp, z)$ due to the interaction between an electron and the AlN-layer quasi-confined-optical-phonon modes for the AlN(100 nm)/GaN(5 nm)/AlN(100 nm) symmetric single QW. For simplicity, we will only consider the $n = 1, 2, 3, 4$ modes. We can see from Figures 5 and 6 that $\Gamma(q_\perp, z)$ has exact symmetry with respect to the center of the QW structure at $z = 2.5$ nm for a given quasi-confined-optical-phonon mode. Both the real and imaginary parts of $\Gamma(q_\perp, z)$ are symmetric for the $n = 1, 3, \ldots$ modes, and antisymmetric for the other modes with $n = 2, 4, \ldots$ The coupling function $\Gamma(q_\perp, z)$ has the oscillation behavior in the AlN layers. The oscillation period is reduced with the increase of the quantum number n. Furthermore, compared with the real (imaginary) part, the imaginary (real) part is so small that we can ignore its contribution to the $|\Gamma(q_\perp, z)|$ for the AlN-layer lower (higher) frequency quasi-confined-optical-phonon modes.

Figures 7 and 8 show the absolute values of $\Gamma(q_\perp, z)$ for the AlN-layer quasi-confined-optical-phonon modes. Our calculations indicate that the electron-quasi-confined-phonon interactions are important for the modes with small quantum number ($n = 1, 2 \ldots, 8$) and can be neglected for all the other modes. For clarity, we will limit

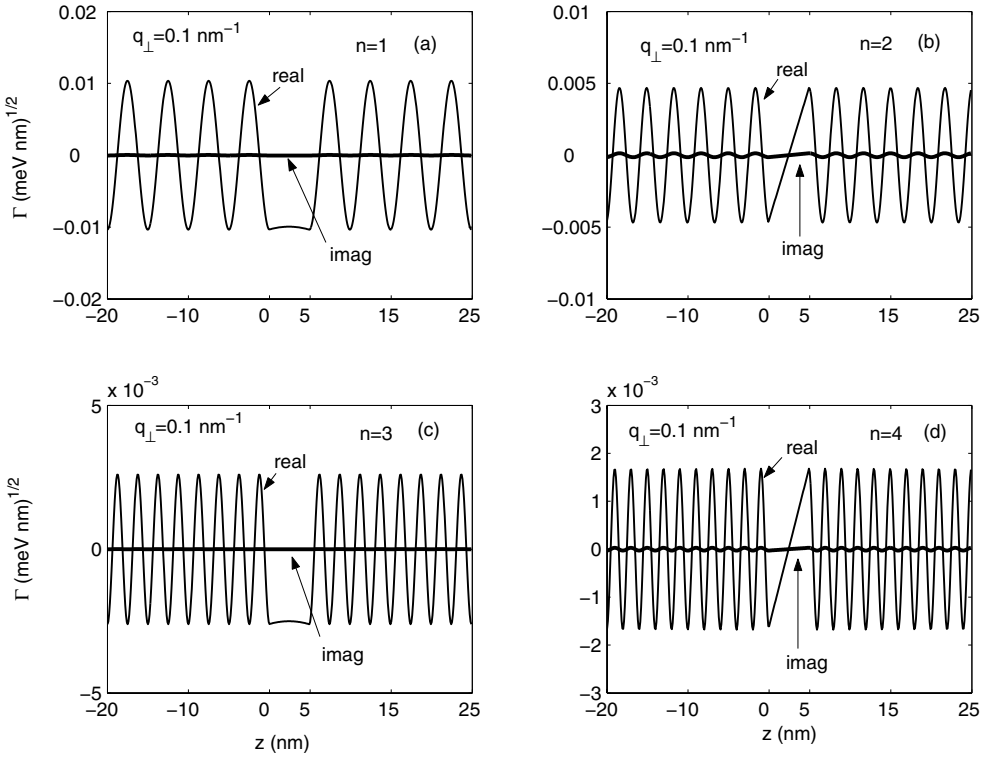

Fig. 5. Spatial dependence of the coupling function $\Gamma(q_\perp, z)$ divided by $(\hbar e^2/8A\varepsilon_0)^{1/2}$ for the interactions between an electron and the AlN-layer lower frequency quasi-confined-optical-phonon modes with the quantum number $n = 1, 2, 3, 4$ and the wave number $q_\perp = 0.1$ nm^{-1} for the AlN/GaN/AlN symmetric single QW with the GaN well layer thickness of $d = 5$ nm and the AlN barrier layer thickness of 100 nm. The heterointerfaces are located at $z = 0$ and 5 nm, respectively. Here the thin (thick) lines are for the real (imaginary) part of $\Gamma(q_\perp, z)$.

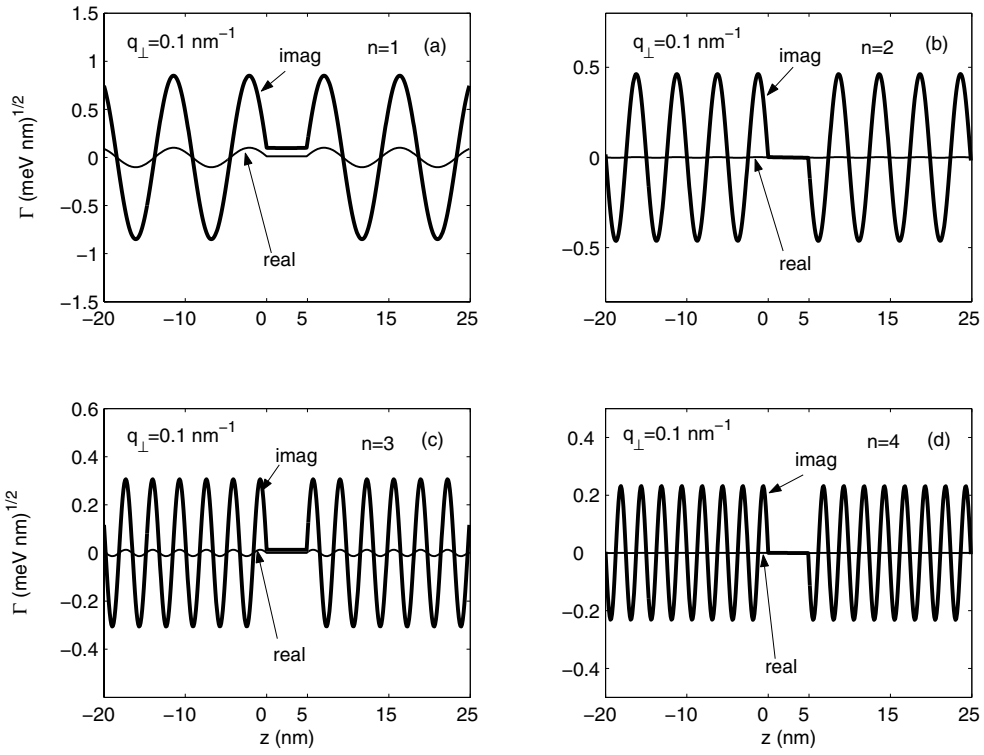

Fig. 6. Same as in Figure 5, but for the AlN-layer higher frequency quasi-confined-optical-phonon modes.

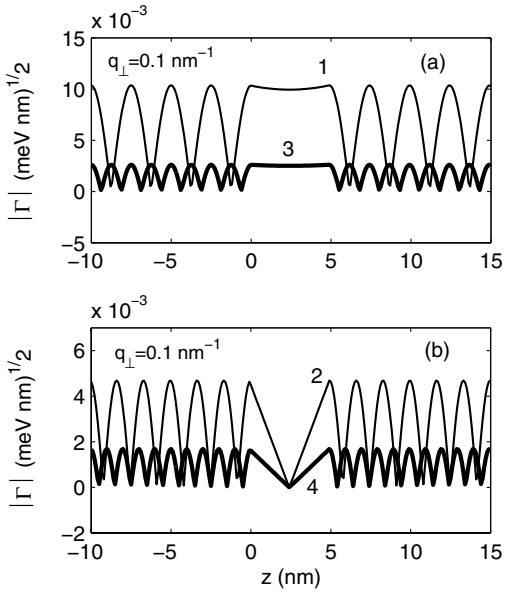

Fig. 7. Absolute values $|\Gamma(q_\perp, z)|$ divided by $(\hbar e^2/8A\varepsilon_0)^{1/2}$ as a function of z for the same QW structure as in Figure 5 for the AlN-layer lower frequency quasi-confined-optical-phonon modes with the quantum number $n = 1, 2, 3, 4$. Here the phonon wave number $q_\perp = 0.1$ nm^{-1}.

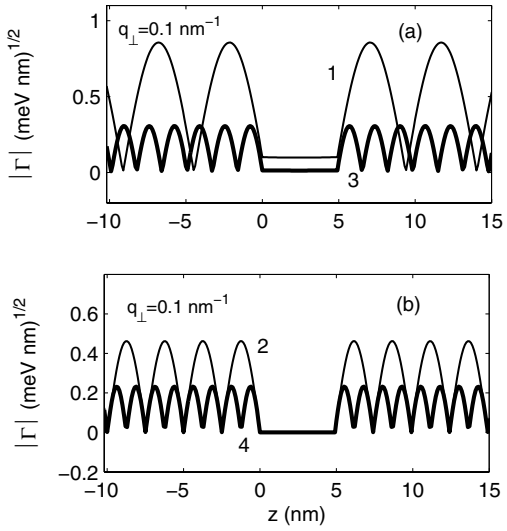

Fig. 8. Same as in Figure 7, but for the AlN-layer higher frequency quasi-confined-optical-phonon modes.

our attention to the modes with the quantum number $n = 1, 2, 3, 4$. We can see from Figures 7 and 8 that the strength of the electron-quasi-confined-phonon interactions is reduced with the increase of the quantum number. Moreover, the electron-quasi-confined-phonon interactions for the $n = 1, 3, \ldots$ symmetric modes are important in both the GaN well layer and the AlN barrier layer. On the contrary, the $n = 2, 4, \ldots$ antisymmetric modes are significant only in the AlN barrier layer. Generally, the electron-phonon interactions due to the higher-frequency modes are much more important than those due to the lower-frequency modes.

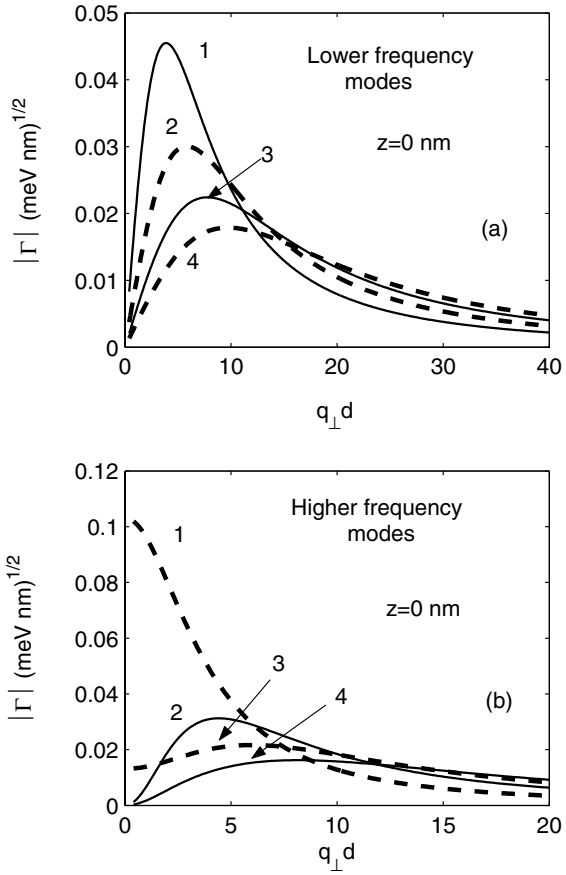

Fig. 9. Absolute values $|\Gamma(q_\perp, z)|$ divided by $(\hbar e^2/8A\varepsilon_0)^{1/2}$ as a function of $q_\perp$ for the same QW structure as in Figure 5. Here (a) is for the lower frequency modes, and (b) for the higher frequency modes.

In Figure 9, we show the absolute values $|\Gamma(q_\perp, z)|$ as a function of wave number $q_\perp$ for the same QW structure as in Figure 5. Figure 9 indicates that the long-wavelength AlN-layer quasi-confined-optical-phonon modes are much more important for their electron-quasi-confined-phonon interactions than the short-wavelength ones. Moreover, we can also see from Figure 9 that the electron-quasi-confined-phonon interactions in the higher frequency range are stronger than those in the lower frequency range.

5 Conclusions

Within the framework of the DC model and Loudon's uniaxial crystal model, we have solved the quasi-confined-optical-phonon modes in a wurtzite Q2D GaN/AlN multilayer heterostructure with an arbitrary number of layers. The p-polarization eigenvector, the dispersion relation and the electron-quasi-confined-phonon interaction Fröhlich-like Hamiltonian are derived using the transfer-matrix method. Our analytical formulas are universal, and can be directly applied to single/multiple QW's and SL's composed of group-III nitrides. For an AlN/GaN/AlN

symmetric single QW, our calculations show that there are infinite quasi-confined-optical-phonon branches, denoted by a quantum number n ($n = 1, 2, \ldots$), with exact symmetry with respect to the center of the QW. The dispersions of the quasi-confined-optical-phonon modes with smaller quantum number n are more significant than for larger n. Moreover, the modes with smaller n are much more important for the electron-quasi-confined-phonon interactions. Generally, it is enough to take into account the modes with $n = 1, 2, \ldots, 8$. The long-wavelength modes are much more important for the electron-quasi-confined-phonon interactions. The electron-phonon interactions due to the higher-frequency modes are much larger than those due to the lower-frequency modes. The oscillation period of the electron phonon coupling function $\Gamma(q_\perp, z)$ is reduced with the increase of the quantum number n. Furthermore, the strain effects of the QW structure have an obvious influence on the dispersions of the GaN-layer quasi-confined-optical-phonon modes and their electron-quasi-confined-phonon interactions. The strength of the GaN-layer electron-quasi-confined-phonon interactions for the lower frequency modes is obviously enhanced due to the strains of the QW structures. The influence of the strains of the QW structure can be neglected for the higher frequency modes. The influence of the strains of the QW structure on the AlN-layer quasi-confined-optical-phonon dispersion and their electron-quasi-confined-phonon interactions can also be ignored. These conclusions are important and useful for further experimental and theoretical investigations of the optical properties and the polaron effects, and for device applications based on the quantum heterostructures of group III nitrides.

This work was supported by the National Natural Science Foundation of China under Grant Nos. 60276004 and 60390073, and by the Scientific Research Foundation for the Returned Overseas Chinese Scholars, State Education Ministry of China.

Appendix A: Electron phonon coupling function for the GaN-layer quasi-confined-optical-phonon modes

For simplicity, we introduce two accessorial functions as follows,

$$\zeta_{\pm,\mathrm{j}} \equiv \frac{1 \pm \gamma_\mathrm{j}}{q_\perp \pm q_{z,\mathrm{j}}},$$

$$\zeta^{(i)}_{\pm,\mathrm{j}} \equiv \frac{1 \pm i\gamma_\mathrm{j}}{q_\perp \pm i q_{z,\mathrm{j}}}, \tag{A.1}$$

and

$$\tau_{\pm,\pm}(x, y, j) = e^{\pm q_\perp (x - z_{j-1})} - e^{\pm q_{z,\mathrm{j}} (y - z_{j-1})},$$

$$\tau^{(i)}_{\pm,\pm}(x, y, j) = e^{\pm q_\perp (x - z_{j-1})} - e^{\pm i q_{z,\mathrm{j}} (y - z_{j-1})}. \tag{A.2}$$

They have the following characteristics,

$$\tau^{(i)}_{+,-}(z_0, z_0, 1) = 0,$$

$$\tau_{-,+}(\infty, z_j, j+1) = -1.$$

The function $f_i(q_\perp, z)$ ($i = 1, 2, 3$) in equation (33) can be written as

$$\begin{aligned} f_1(q_\perp, z) = {} & -\zeta_{+,0}\Big[\tau_{+,+}(z_0, z, 1) - 1\Big] \\ & + \zeta_{-,0}\tau_{+,+}(z, z, 1) \\ & + \sum_{j=1,3,5\cdots}^{N} \Big\{\Big[- A^*_j \zeta^{(i)}_{+,\mathrm{j}} \tau^{(i)}_{-,+}(z_j, z_j, j) \\ & - B^*_j \zeta^{(i)}_{-,\mathrm{j}} \tau^{(i)}_{-,-}(z_j, z_j, j)\Big]\Big[1 + \tau_{+,+}(z, z_{j-1}, j)\Big]\Big\} \\ & + \sum_{j=2,4,6\cdots}^{N-1} \Big\{\Big[- A^*_j \zeta_{+,\mathrm{j}} \tau_{-,+}(z_j, z_j, j) \\ & + B^*_j \zeta_{-,\mathrm{j}} \tau_{-,-}(z_j, z_j, j)\Big]\Big[1 + \tau_{+,+}(z, z_{j-1}, j)\Big]\Big\} \\ & + A^*_{N+1}\zeta_{+,N+1}\Big[\tau_{+,+}(z, z_N, N+1) + 1\Big], \end{aligned} \tag{A.3}$$

$$\begin{aligned} f_{2,\mathrm{GaN}}(q_\perp, z) = {} & \zeta_{+,0}\Big[\tau_{-,+}(z, z_0, 1) + 1\Big] \\ & + \sum_{m=1,3,5\cdots}^{j-2} \Big\{\Big[A^*_m \zeta^{(i)}_{-,\mathrm{m}} \tau^{(i)}_{+,+}(z_m, z_m, m) \\ & + B^*_m \zeta^{(i)}_{+,\mathrm{m}} \tau^{(i)}_{+,-}(z_m, z_m, m)\Big]\Big[1 + \tau^{(i)}_{-,+}(z, z_{m-1}, m)\Big]\Big\} \\ & + \sum_{m=2,4,6\cdots}^{j-1} \Big\{\Big[A^*_m \zeta_{-,m} \tau_{+,+}(z_m, z_m, m) \\ & + B^*_m \zeta_{+,m} \tau_{+,-}(z_m, z_m, m)\Big]\Big[1 + \tau_{-,+}(z, z_{m-1}, m)\Big]\Big\} \\ & + \Big[A^*_j \zeta^{(i)}_{-,\mathrm{j}} \tau^{(i)}_{+,+}(z, z, j) \\ & + B^*_j \zeta^{(i)}_{+,\mathrm{j}} \tau^{(i)}_{+,-}(z, z, j)\Big]\Big[\tau^{(i)}_{-,+}(z, z_{j-1}, j) + 1\Big] \\ & + \sum_{\mathrm{m=j+1,j+3}\cdots}^{N-1} \Big\{\Big[- A^*_m \zeta_{+,\mathrm{m}} \tau_{-,+}(z_m, z_m, m) \\ & + B^*_m \zeta_{-,\mathrm{m}} \tau_{-,-}(z_m, z_m, m)\Big]\Big[1 + \tau_{+,+}(z, z_{m-1}, m)\Big]\Big\} \\ & + \sum_{\mathrm{m=j+2,j+4}\cdots}^{N} \Big\{\Big[- A^*_m \zeta^{(i)}_{+,\mathrm{m}} \tau^{(i)}_{-,+}(z_m, z_m, m) \\ & - B^*_m \zeta^{(i)}_{-,\mathrm{m}} \tau^{(i)}_{-,-}(z_m, z_m, m)\Big]\Big[1 + \tau_{+,+}(z, z_{m-1}, m)\Big]\Big\} \\ & + A^*_{N+1}\zeta_{+,N+1}\Big[\tau_{+,+}(z, z_N, N+1) + 1\Big], \end{aligned} \tag{A.4}$$

$$
\begin{aligned}
f_{2,\mathrm{AlN}}(q_\perp,z) &= \zeta_{+,0}\Big[\tau_{-,+}(z,z_0,1)+1\Big] \\
&+\sum_{m=1,3,5\cdots}^{j-1}\Big\{\Big[A_m^*\zeta_{-,\mathrm{m}}^{(i)}\tau_{+,+}^{(i)}(z_m,z_m,m) \\
&+B_m^*\zeta_{+,\mathrm{m}}^{(i)}\tau_{+,-}^{(i)}(z_m,z_m,m)\Big]\Big[1+\tau_{-,+}^{(i)}(z,z_{m-1},m)\Big]\Big\} \\
&+\sum_{m=2,4,6\cdots}^{j-2}\Big\{\Big[A_m^*\zeta_{-,m}\tau_{+,+}(z_m,z_m,m) \\
&+B_m^*\zeta_{+,m}\tau_{+,-}(z_m,z_m,m)\Big]\Big[1+\tau_{-,+}(z,z_{m-1},m)\Big]\Big\} \\
&+A_j^*\zeta_{-,j}\tau_{+,-}(z,z,j)\Big[\tau_{+,+}(z_{j-1},z_j,j)-1\Big] \\
&+B_j^*\zeta_{+,j}\tau_{-,+}(z,z,j)\Big[\tau_{+,-}(z_{j-1},z_j,j)-1\Big] \\
&+\sum_{\mathrm{m=j+2,j+4\cdots}}^{N-1}\Big\{\Big[-A_m^*\zeta_{+,\mathrm{m}}\tau_{-,+}(z_m,z_m,m) \\
&+B_m^*\zeta_{-,\mathrm{m}}\tau_{-,-}(z_m,z_m,m)\Big]\Big[1+\tau_{+,+}(z,z_{m-1},m)\Big]\Big\} \\
&+\sum_{\mathrm{m=j+1,j+3\cdots}}^{N}\Big\{\Big[-A_m^*\zeta_{+,\mathrm{m}}^{(i)}\tau_{-,+}^{(i)}(z_m,z_m,m) \\
&-B_m^*\zeta_{-,\mathrm{m}}^{(i)}\tau_{-,-}^{(i)}(z_m,z_m,m)\Big]\Big[1+\tau_{+,+}(z,z_{m-1},m)\Big]\Big\} \\
&+A_{N+1}^*\zeta_{+,N+1}\Big[\tau_{+,+}(z,z_N,N+1)+1\Big],
\end{aligned}
\tag{A.5}
$$

$$
\begin{aligned}
f_3(q_\perp,z) &= \zeta_{+,0}\Big[\tau_{-,+}(z,z_0,1)+1\Big] \\
&+\sum_{j=1,3,5\cdots}^{N}\Big[A_j^*\zeta_{-,\mathrm{j}}^{(i)}\tau_{+,+}^{(i)}(z_j,z_j,j) \\
&+B_j^*\zeta_{+,\mathrm{j}}^{(i)}\tau_{+,-}^{(i)}(z_j,z_j,j)\Big]\Big[1+\tau_{-,+}^{(i)}(z,z_{j-1},j)\Big] \\
&+\sum_{j=2,4,6\cdots}^{N-1}\Big\{\Big[A_j^*\zeta_{-,j}\tau_{+,+}(z_j,z_j,j) \\
&+B_j^*\zeta_{+,j}\tau_{+,-}(z_j,z_j,j)\Big]\Big[1+\tau_{-,+}(z,z_{j-1},j)\Big]\Big\} \\
&-A_{N+1}^*\zeta_{-,N+1}\tau_{-,-}(z,z,N+1) \\
&-A_{N+1}^*\zeta_{-,N+1}\Big[\tau_{-,-}(z_N,z,N+1)-1\Big].
\end{aligned}
\tag{A.6}
$$

Appendix B: Electron phonon coupling function for the AlN-layer quasi-confined-optical-phonon modes

Similarly, the corresponding functions of $f_i(q_\perp,z)$ $(i=1,2,3)$ for the coupling between an electron and the AlN-layer quasi-confined-optical-phonon modes can be derived as,

$$
\begin{aligned}
f_1(q_\perp,z) &= -B_0^*\Big[\zeta_{+,0}^{(i)}\tau_{+,+}^{(i)}(-\infty,z,1) \\
&+\zeta_{-,0}^{(i)}\tau_{+,+}^{(i)}(z,z,1)-\zeta_{+,0}^{(i)}\tau_{+,-}^{(i)}(z,z,1) \\
&-\zeta_{-,0}^{(i)}\tau_{+,-}^{(i)}(-\infty,z,1)\Big]+\sum_{j=1,3,5\cdots}^{N}\Big\{\Big[-A_j^*\zeta_{+,\mathrm{j}}\tau_{-,+}(z_j,z_j,j) \\
&+B_j^*\zeta_{-,\mathrm{j}}\tau_{-,-}(z_j,z_j,j)\Big]\Big[1+\tau_{+,+}(z,z_{j-1},j)\Big]\Big\} \\
&+\sum_{j=2,4,6\cdots}^{N-1}\Big\{\Big[-A_j^*\zeta_{+,\mathrm{j}}^{(i)}\tau_{-,+}^{(i)}(z_j,z_j,j) \\
&-B_j^*\zeta_{-,\mathrm{j}}^{(i)}\tau_{-,-}^{(i)}(z_j,z_j,j)\Big]\Big[1+\tau_{+,+}(z,z_{j-1},j)\Big]\Big\} \\
&+\Big[A_{N+1}^*\zeta_{+,N+1}^{(i)}+B_{N+1}^*\zeta_{-,N+1}^{(i)}\Big]\Big[1+\tau_{+,+}(z,z_N,N+1)\Big],
\end{aligned}
\tag{B.1}
$$

$$
\begin{aligned}
f_{2,\mathrm{GaN}}(q_\perp,z) &= \Big[\zeta_{-,0}^{(i)}+B_0^*\zeta_{+,0}^{(i)}\Big]\Big[1+\tau_{-,+}^{(i)}(z,z_0,1)\Big] \\
&+\sum_{m=1,3,5\cdots}^{j-2}\Big\{\Big[A_m^*\zeta_{-,m}\tau_{+,+}(z_m,z_m,m) \\
&+B_m^*\zeta_{+,m}\tau_{+,-}(z_m,z_m,m)\Big]\Big[1+\tau_{-,+}(z,z_{m-1},m)\Big]\Big\} \\
&+\sum_{m=2,4,6\cdots}^{j-1}\Big[A_m^*\zeta_{-,\mathrm{m}}^{(i)}\tau_{+,+}^{(i)}(z_m,z_m,m) \\
&+B_m^*\zeta_{+,\mathrm{m}}^{(i)}\tau_{+,-}^{(i)}(z_m,z_m,m)\Big]\Big[1+\tau_{-,+}^{(i)}(z,z_{m-1},m)\Big] \\
&+A_j^*\zeta_{-,j}\tau_{+,-}(z,z,j)\Big[\tau_{+,+}(z_{j-1},z_j,j)-1\Big] \\
&+B_j^*\zeta_{+,j}\tau_{-,+}(z,z,j)\Big[\tau_{+,-}(z_{j-1},z_j,j)-1\Big] \\
&+\sum_{\mathrm{m=j+2,j+4\cdots}}^{N}\Big\{\Big[-A_m^*\zeta_{+,\mathrm{m}}\tau_{-,+}(z_m,z_m,m) \\
&+B_m^*\zeta_{-,\mathrm{m}}\tau_{-,-}(z_m,z_m,m)\Big]\Big[1+\tau_{+,+}(z,z_{m-1},m)\Big]\Big\} \\
&+\sum_{\mathrm{m=j+1,j+3\cdots}}^{N-1}\Big\{\Big[-A_m^*\zeta_{+,\mathrm{m}}^{(i)}\tau_{-,+}^{(i)}(z_m,z_m,m) \\
&-B_m^*\zeta_{-,\mathrm{m}}^{(i)}\tau_{-,-}^{(i)}(z_m,z_m,m)\Big]\Big[1+\tau_{+,+}(z,z_{m-1},m)\Big]\Big\} \\
&+\Big[A_{N+1}^*\zeta_{+,N+1}^{(i)}+B_{N+1}^*\zeta_{-,N+1}^{(i)}\Big]\Big[1+\tau_{+,+}(z,z_N,N+1)\Big],
\end{aligned}
\tag{B.2}
$$

$$
\begin{aligned}
f_{2,\mathrm{AlN}}(q_\perp,z) &= \left[\zeta^{(i)}_{-,0} + B^*_0\zeta^{(i)}_{+,0}\right]\left[1+\tau^{(i)}_{-,+}(z,z_0,1)\right] \\
&+ \sum_{m=1,3,5\cdots}^{j-1}\Big\{\Big[A^*_m\zeta_{-,m}\tau_{+,+}(z_m,z_m,m) \\
&+B^*_m\zeta_{+,m}\tau_{+,-}(z_m,z_m,m)\Big]\Big[1+\tau_{-,+}(z,z_{m-1},m)\Big]\Big\} \\
&+ \sum_{m=2,4,6\cdots}^{j-2}\Big\{\Big[A^*_m\zeta^{(i)}_{-,\mathrm{m}}\tau^{(i)}_{+,+}(z_m,z_m,m) \\
&+B^*_m\zeta^{(i)}_{+,\mathrm{m}}\tau^{(i)}_{+,-}(z_m,z_m,m)\Big]\Big[1+\tau^{(i)}_{-,+}(z,z_{m-1},m)\Big]\Big\} \\
&+\Big[A^*_j\zeta^{(i)}_{-,\mathrm{j}}\tau^{(i)}_{+,+}(z,z,j) \\
&+B^*_j\zeta^{(i)}_{+,\mathrm{j}}\tau^{(i)}_{+,-}(z,z,j)\Big]\Big[\tau^{(i)}_{-,+}(z,z_{j-1},j)+1\Big] \\
&+ \sum_{\mathrm{m=j+2,j+4}\cdots}^{N}\Big\{\Big[-A^*_m\zeta_{+,\mathrm{m}}\tau_{-,+}(z_m,z_m,m) \\
&+B^*_m\zeta_{-,\mathrm{m}}\tau_{-,-}(z_m,z_m,m)\Big]\Big[1+\tau_{+,+}(z,z_{m-1},m)\Big]\Big\} \\
&+ \sum_{\mathrm{m=j+1,j+3}\cdots}^{N-1}\Big\{\Big[-A^*_m\zeta^{(i)}_{+,\mathrm{m}}\tau^{(i)}_{-,+}(z_m,z_m,m) \\
&-B^*_m\zeta^{(i)}_{-,\mathrm{m}}\tau^{(i)}_{-,-}(z_m,z_m,m)\Big]\Big[1+\tau_{+,+}(z,z_{m-1},m)\Big]\Big\} \\
&+\Big[A^*_{N+1}\zeta^{(i)}_{+,N+1} + B^*_{N+1}\zeta^{(i)}_{-,N+1}\Big]\Big[1+\tau_{+,+}(z,z_N,N+1)\Big],
\end{aligned}
\tag{B.3}
$$

$$
\begin{aligned}
f_3(q_\perp,z) &= \left[\zeta^{(i)}_{-,0} + B^*_0\zeta^{(i)}_{+,0}\right]\left[1+\tau^{(i)}_{-,+}(z,z_0,1)\right] \\
&+ \sum_{j=1,3,5\cdots}^{N}\Big\{\Big[A^*_j\zeta_{-,j}\tau_{+,+}(z_j,z_j,j) \\
&+B^*_j\zeta_{+,j}\tau_{+,-}(z_j,z_j,j)\Big]\Big[1+\tau_{-,+}(z,z_{j-1},j)\Big]\Big\} \\
&+ \sum_{j=2,4,6\cdots}^{N-1}\Big[A^*_j\zeta^{(i)}_{-,\mathrm{j}}\tau^{(i)}_{+,+}(z_j,z_j,j) \\
&+B^*_j\zeta^{(i)}_{+,\mathrm{j}}\tau^{(i)}_{+,-}(z_j,z_j,j)\Big]\Big[1+\tau^{(i)}_{-,+}(z,z_{j-1},j)\Big] \\
&-A^*_{N+1}\zeta^{(i)}_{-,N+1}\tau^{(i)}_{-,-}(z,z,N+1) \\
&-B^*_{N+1}\zeta^{(i)}_{+,N+1}\tau^{(i)}_{-,+}(z,z,N+1) \\
&+A^*_{N+1}\zeta^{(i)}_{+,N+1}\Big[\tau^{(i)}_{+,+}(z,z_N,N+1)+1\Big] \\
&+B^*_{N+1}\zeta^{(i)}_{-,N+1}\Big[\tau^{(i)}_{+,+}(z,z_N,N+1)+1\Big].
\end{aligned}
\tag{B.4}
$$

References

1. S. Nakamura, G. Fasol, *The Blue Laser Diode* (Berlin, Springer-Verlag, 1997)
2. B. Gil, *Group III Nitride Semiconductor Compounds* (Oxford, Clarendon, 1998)
3. O. Ambacher, J. Phys. D: Appl. Phys. **31**, 2653 (1998)
4. S. Nakamura, Science **281**, 956 (1998)
5. S.C. Jain, M. Willander, J. Narayan, R.V. Overstraeten, J. Appl. Phys. **87**, 965 (2000)
6. S. Nakamura, S.F. Chichibu, *Introduction to Nitride Semiconductor Blue Lasers and Light Emitting Diodes* (London, Taylor & Francis, 2000)
7. Jun-jie Shi, Solid State Commun. **124**, 341 (2002)
8. Jun-jie Shi, Zi-zhao Gan, J. Appl. Phys. **94**, 407 (2003)
9. Jun-jie Shi, Phys. Rev. B **68**, 165335 (2003)
10. Jun-jie Shi, Solid State Commun. **127**, 51 (2003)
11. Jun-jie Shi, Xing-li Chu, E.M. Goldys, Phys. Rev. B **70**, 115318 (2004)
12. B.C. Lee, K.W. Kim, M.A. Stroscio, M. Dutta, Phys. Rev. B **58**, 4860 (1998)
13. S.M. Komirenko, K.W. Kim, M.A. Stroscio, M. Dutta, Phys. Rev. B **59**, 5013 (1999)
14. J. Gleize, M.A. Renucci, J. Frandon, F. Demangeot, Phys. Rev. B **60**, 15985 (1999)
15. L. Wendler, Phys. Status Solidi (b) **129**, 513 (1985)
16. L. Wendler, R. Pechstedt, Phys. Status Solidi (b) **141**, 129 (1987)
17. L. Wendler, R. Haupt, Phys. Status Solidi (b) **141**, 493 (1987)
18. L. Wendler, R. Haupt, Phys. Status Solidi (b) **143**, 487 (1987)
19. Jun-jie Shi, Ling-xi Shangguan, Shao-hua Pan, Phys. Rev. B **47**, 13471 (1993)
20. Jun-jie Shi, Shao-hua Pan, Phys. Rev. B **51**, 17681 (1995)
21. Jun-jie Shi, Shao-hua Pan, J. Appl. Phys. **80**, 3863 (1996)
22. Jun-jie Shi, B.C. Sanders, Shao-hua Pan, E.M. Goldys, Phys. Rev. B **60**, 16031 (1999)
23. R. Loudon, Adv. Phys. **13**, 423 (1964)
24. W. Hayes, R. Loudon, *Scattering of Light by Crystals* (New York, Wiley, 1978), p. 169
25. S.M. Komirenko, K.W. Kim, M.A. Stroscio, M. Dutta, Phys. Rev. B **61**, 2034 (2000)
26. B.C. Lee, K.W. Kim, M. Dutta, M.A. Stroscio, Phys. Rev. B **56**, 997 (1997)
27. M.E. Mora-Ramos, F.J. Rodríguez, L. Quiroga, J. Phys.: Condens. Matter **11**, 8223 (1999)
28. M.E. Mora-Ramos, Phys. Status Solidi (b) **219**, R1 (2000)
29. M.E. Mora-Ramos, Phys. Status Solidi (b) **223**, 843 (2001)
30. D. Romanov, V. Mitin, M. Stroscio, Physica B **316-317**, 359 (2002)
31. D.A. Romanov, V.V. Mitin, M.A. Stroscio, Phys. Rev. B **66**, 115321 (2002)
32. D. Romanov, V. Mitin, M. Stroscio, Physica E **12**, 491 (2002)
33. J. Gleize, F. Demangeot, J. Frandon, M.A. Renucci, M. Kuball, B. Daudin, N. Grandjean, Phys. Status Solidi (a) **183**, 157 (2001)
34. J. Gleize, J. Frandon, F. Demangeot, M.A. Renucci, M. Kuball, J.M. Hayes, F. Widmann, B. Daudin, Mater. Sci. Eng., B **82**, 27 (2001)
35. S.J. Xu, W. Liu, M.F. Li, Appl. Phys. Lett. **77**, 3376 (2000)
36. L. Bergman, D. Alexson, P.L. Murphy, R.J. Nemanich, M. Dutta, M.A. Stroscio, C. Balkas, H. Shin, R.F. Davis, Phys. Rev. B **59**, 12977 (1999)
37. D. Alexson, L. Bergman, M. Dutta, K.W. Kim, S. Komirenko, R.J. Nemanich, B.C. Lee, M.A. Stroscio, S. Yu, Physica B **263-264**, 510 (1999)
38. H. Haken, *Quantum Field Theory of Solids* (Amsterdam, North-Holland, 1976)